POLITECNICO DI TORINO
Repository ISTITUZIONALE

A multi-phase shaking table dataset of reinforced concrete frames retrofitted with a timber–aluminium exoskeleton

Original
A multi-phase shaking table dataset of reinforced concrete frames retrofitted with a timber–aluminium exoskeleton / Shoklarovski, A., Sheshov, V., Rakicevic, Z., Bogdanovic, A., Manojlovski, F., Poposka, A., Bojadjieva, J., Ivanovski, D., Kitanovski, T., Markovski, I., Filipovski, D., Naumovski, N., Meglio, E., Domaneschi, M., Cucuzza, R., Villa, V., Marano, G.C., Formisano, A.. - In: SCIENTIFIC DATA. - ISSN 2052-4463. - (2026), pp. 1-17. [10.1038/s41597-026-08409-3]

Availability:
This version is available at: 11583/3017072 since: 2026-10-27T14:14:08Z

Publisher:
Springer Nature

Published
DOI:10.1038/s41597-026-08409-3

Terms of use:

This article is made available under terms and conditions as specified in the corresponding bibliographic description in the repository

Publisher copyright

(Article begins on next page)

26 November 2026

scientific data

Article in Press

Check for updates

OPEN

DATA DESCRIPTOR

A multi-phase shaking table dataset of reinforced concrete frames retrofitted with a timber–aluminium exoskeleton

Antonio Shoklarovski[1]✉, Vlatko Sheshov[1], Zoran Rakicevic[1], Aleksandra Bogdanovic[1], Filip Manojlovski[1], Angela Poposka[1], Julijana Bojadjieva[1], Dejan Ivanovski[1], Toni Kitanovski[1], Igor Markovski[1], Dejan Filipovski[1], Nikola Naumovski[1], Emilia Meglio[2], Marco Domaneschi[3]✉, Raffaele Cucuzza[3], Valentina Villa[3], Giuseppe Carlo Marano[3] & Antonio Formisano[2]

A significant portion of the existing reinforced concrete (RC) building stock in Europe was designed according to outdated standards and is vulnerable both to earthquake damage and to poor energy performance. Retrofit solutions that integrate structural strengthening with envelope upgrading have therefore emerged as a promising strategy to address safety and decarbonisation objectives simultaneously. Within this context, the EU-funded Horizon Europe project Engineering Research Infrastructures for European Synergies (ERIES) supported the REsilient and SUstainable envelope for vulnerable buildings in seisMic affected areas at the time of climatE crisis (RESUME) project, which investigated the seismic response of RC frames strengthened with a hybrid timber–aluminium exoskeleton system incorporating prefabricated façade panels for thermal upgrading. To investigate seismic vulnerability, two geometrically scaled (1:3) two-storey RC frame specimens representative of non-ductile typologies were constructed and tested on a shaking table at the Institute of Earthquake Engineering and Engineering Seismology (IZIIS), North Macedonia. The experimental campaign comprised 66 shaking table tests conducted in three phases. The dataset includes synchronised time-history measurements of accelerations, displacements and strains, together with input ground motions and detailed metadata describing geometry, materials, instrumentation and testing sequence. The data support validation of numerical models and comparative assessment of structural retrofit configurations within an integrated retrofit framework.

Background & Summary

In recent decades, the construction sector in Europe has increasingly shifted its focus from new construction to the renovation and upgrading of the existing building stock. This transition has been driven by two parallel challenges: the high seismic vulnerability of ageing structures and the urgent need to improve their energy efficiency in response to climate change[1–4].

A significant portion of reinforced concrete (RC) buildings in Europe was constructed before the introduction of modern seismic design regulations. Consequently, many of these structures lack adequate detailing and capacity-design provisions, resulting in limited ductility and increased seismic vulnerability. Observations from recent earthquakes have repeatedly confirmed the susceptibility of this non-ductile building stock to structural and non-structural damage[2–4].

At the same time, the building sector accounts for approximately 35% of global energy consumption and 38% of greenhouse gas emissions[5]. International and European policy frameworks, including the European Green

[1]Institute of Earthquake Engineering and Engineering Seismology (IZIIS), University "Ss. Cyril and Methodius", Skopje, Republic of North Macedonia. [2]Department of Structures for Engineering and Architecture, University of Naples Federico II, Naples, Italy. [3]Department of Structural, Building and Geotechnical Engineering, Politecnico di Torino, Turin, Italy. ✉e-mail: antonio@iziis.ukim.edu.mk; marco.domaneschi@polito.it

Deal, promote large-scale renovation programmes aimed at improving sustainability and reducing environmental impact[6–9]. However, current renovation rates remain insufficient to achieve the required targets for energy efficiency and resilience[6]. For this reason, recent research has emphasised the importance of integrated approaches that combine seismic strengthening with energy upgrading, rather than treating these aspects as separate interventions[10–14].

Among the various retrofit strategies proposed in the literature, external façade-based systems have attracted increasing attention. Compared with internal strengthening interventions, these systems minimise disruption to occupants, preserve the usable floor area, and allow retrofit works to be performed while maintaining building functionality. These characteristics make them particularly suitable for the renovation of existing residential buildings. These include textile- and fibre-reinforced solutions combined with insulation layers[15–18], prefabricated timber-based façade systems[19–24], and steel or hybrid exoskeleton configurations[25–31]. Exoskeleton systems are independent structural systems positioned externally to the primary load-bearing structure and connected to it in order to enhance global stability and deformation capacity while allowing architectural and functional integration[25–31]. More recently, lightweight metal shear panels, including aluminium panels, have been investigated as façade-based seismic upgrading components[32,33].

While timber- and aluminium-based retrofit systems have previously been investigated independently, fewer studies have considered their combined application within a single external retrofit solution. In the RESUME project, laminated timber members provide the primary supporting frame for prefabrication and rapid installation, whereas aluminium shear panels contribute to the lateral load-resisting mechanism. The cork insulation layer complements the structural intervention by providing thermal insulation, allowing the proposed solution to address both seismic safety and energy efficiency within a single retrofit concept.

The Engineering Research Infrastructures for European Synergies (ERIES) project, funded under the Horizon Europe Framework Programme, supports access to large-scale testing facilities and the dissemination of research data[34]. Within this framework, the RESUME project developed and experimentally assessed a hybrid timber–aluminium exoskeleton system for the integrated seismic and energy retrofitting of reinforced concrete frames.

The dataset presented in this paper originates from the multi-phase shaking table campaign conducted within the framework of the RESUME project at the Institute of Earthquake Engineering and Engineering Seismology (IZIIS), Skopje[35–38]. While previous publications arising from this experimental campaign focused primarily on the interpretation of the experimental results, the present contribution provides public access to the complete experimental dataset together with the associated documentation required for its interpretation and reuse. Two geometrically scaled (1:3) two-storey RC frame models, representative of typical pre-1970s non-ductile reinforced concrete buildings, were constructed and tested under controlled dynamic excitation. The prototype was designed to reproduce the main characteristics of existing reinforced concrete buildings designed primarily for gravity loads, with inadequate seismic detailing typical of the pre-code building stock[39]. The experimental programme comprised three structural configurations: an unstrengthened specimen, a post-damage strengthened specimen, and a pre-strengthened specimen, subjected to progressively increasing seismic input.

The dataset comprises synchronised time-history records of acceleration, displacement and strain, together with input motions and documentation of the testing sequence. The complete dataset is publicly available through the Built Environment Data repository and supports future numerical model calibration, comparative assessment of retrofit configurations, and further investigations based on the reported experimental data.

Methods

As-built models. The experimental campaign was conducted at the Institute of Earthquake Engineering and Engineering Seismology (IZIIS), Skopje. The programme involved two geometrically scaled (1:3) reinforced concrete (RC) frame specimens.

Each specimen represents a two-storey structure with a total longitudinal length of 4.2 m. The ground floor height is 1.5 m, while the upper storey height is 1.0 m. The structural system consists of two parallel longitudinal frames spaced 1.4 m apart, connected transversely by the RC slabs and perimeter beams.

Beams have rectangular cross-sections of 10×15 cm and columns are square with 10×10 cm sections. Longitudinal reinforcement consists of Ø8 bars placed at the corners, while transverse reinforcement is provided by Ø4 stirrups spaced at 10 cm.

Hollow brick infill walls (10 cm thick) constructed using B10 clay blocks ($250 \times 250 \times 100$ mm) and MM50 mortar are installed in the end bays along the longitudinal direction. The wall thickness corresponds to the adopted 1:3 geometric scale of the experimental models.

Two RC slabs, each 6 cm thick, are cast at elevations of 1.5 m and 2.5 m. The slabs are reinforced with Ø6 bars spaced at 7 cm in both orthogonal directions in the top and bottom layers. The lower slab includes a central rectangular opening measuring 900×1400 mm, provided for experimental access, whereas the upper slab covers the entire plan area.

The specimens are supported on RC strip footings: 85×25 cm in the longitudinal direction, reinforced with 11Ø10 bars in both top and bottom layers, and 80×25 cm at the transverse ends with 10Ø10 longitudinal bars. All footings include Ø4 stirrups spaced at 10 cm.

The scaling relationships adopted in this study are summarised in Table 1, based on a geometric scale factor of $\lambda = 1{:}3$ and following the principles of similitude theory for reduced-scale dynamic testing[40,41].

To reproduce the target inertial mass, eight steel ingots (≈3.9 kN each, 400 kg) were placed on the upper slab, providing a total additional vertical load of approximately 31 kN. The ingots were restrained against movement in the direction of excitation by steel L-shaped boundary profiles anchored to the slab, while adjacent ingots were interconnected by welded steel plates. The front and rear boundary profiles were additionally connected by two tensioned threaded rods on both sides, ensuring stable positioning of the ingots throughout the testing programme.

Parameter	Scaling factor
Geometric length	$l_r = 1/3$
Time	$t_r = \sqrt{l_r} = \sqrt{1/3}$
Frequency	$\omega_r = \frac{1}{\sqrt{l_r}} = \sqrt{3}$
Mass density	$\rho_r = \frac{E_r}{l_r} = 3$
Modulus of elasticity	$E_r = \frac{E_{model}}{E_{prototype}} = 1$
Self-weight	$M_{str,r} = l_r^3 = \frac{1}{27} \approx 0.037$
Mass	$M_r = E_r l_r^2 \approx 0.11$
Strain	$\varepsilon_r = 1$
Acceleration	$a_r = 1$

Table 1. Scaling factors.

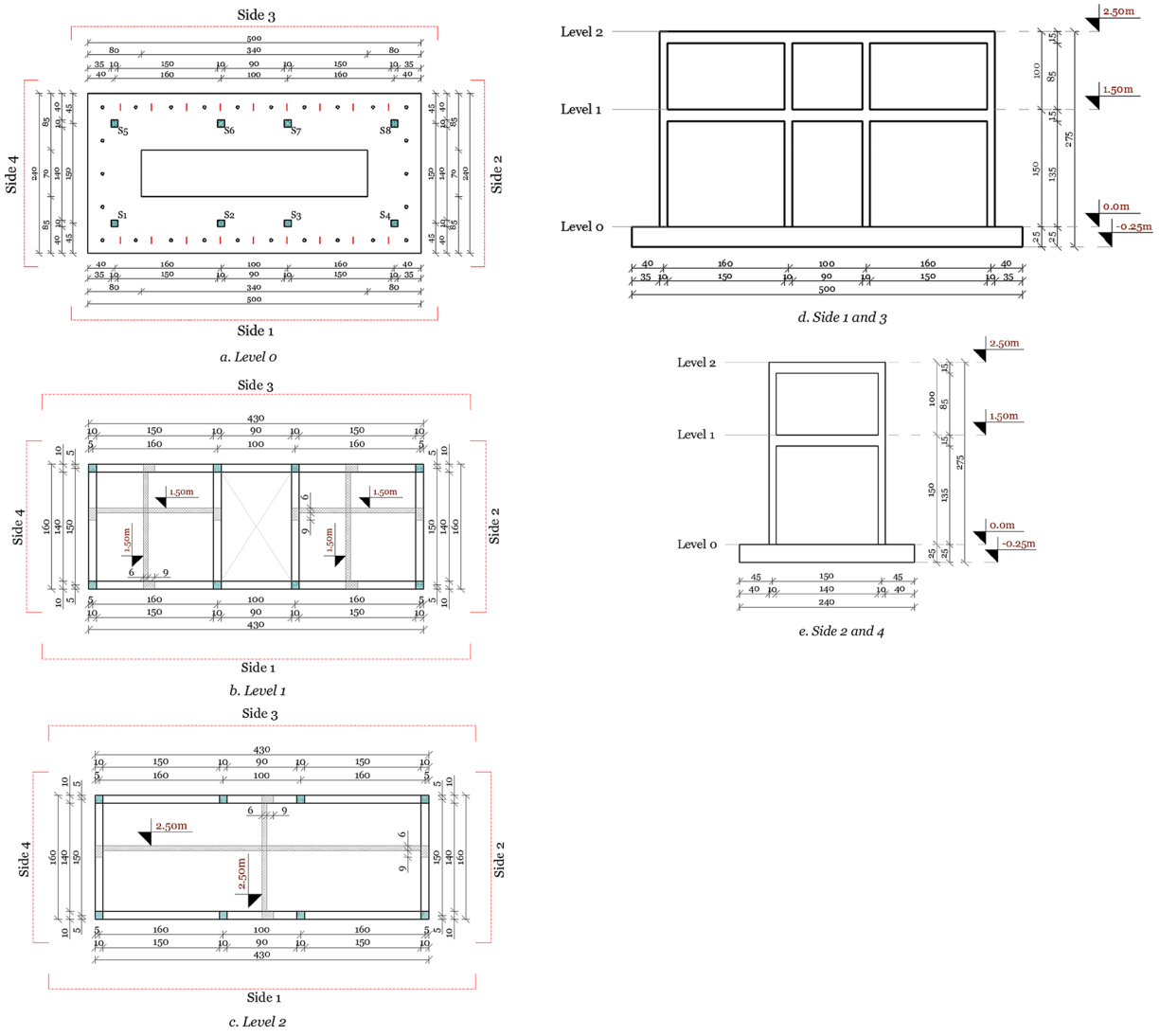


Fig. 1 Technical drawings of the specimens.

Technical drawings of the specimens are provided in Fig. 1, while Fig. 2 shows the unstrengthened specimen. In Fig. 1, labels S1–S8 identify the reinforced concrete columns. The small circles denote the anchor holes used to fix the specimen to the shaking table, whereas the red markers indicate the lifting anchors used for handling the specimen during transportation and installation.

Strengthening solution - Exoskeleton system. The strengthening system consists of a hybrid timber–aluminium exoskeleton applied externally to the reinforced concrete frames. The primary structural elements are

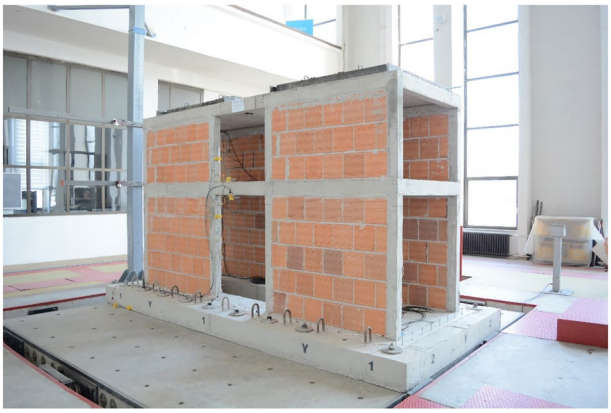


Fig. 2 Unstrengthened RC specimen.

Gl24h laminated timber members connected through galvanised steel plates and mechanical fasteners, forming a shared external frame.

The exoskeleton is connected to the existing RC structure by means of Ø16 mm steel pins fixed to the RC frame at each beam–column joint and at the foundation level. At the beam–column joints, the steel end plates of the timber beams are inserted into local slots formed in the timber columns. Aligned holes in the timber columns and steel end plates allow the steel pins to pass through both elements. Since the pins are fixed only to the RC frame and are not rigidly connected to the steel end plates, the joints behave as pinned connections, allowing relative rotation between the timber frame and the existing RC structure. At the foundation level, the bottom timber beam is seated within continuous steel plates anchored to the RC foundation using Ø10 mm anchor bolts spaced at 200 mm intervals. The timber beam is connected to the steel plates by countersunk Ø4 mm bolts arranged in groups of three at the same spacing, providing a continuous load-transfer path between the exoskeleton and the RC foundation. The system is installed on all exterior façades except for the central longitudinal span, which remains uncovered to allow direct observation during laboratory testing.

The lateral load-resisting mechanism is provided by 2 mm thick aluminium shear panels made of EN AW-5754 H111 alloy. These panels act as dissipative elements, contributing to lateral stiffness and energy dissipation under seismic excitation.

Aluminium panels are connected to the timber frame using galvanised steel angles. The façade system also incorporates a 10 mm thick expanded cork insulation layer (density 108–120 kg/m^3, thermal conductivity 0.0375 W/mK), contributing to the integrated structural and thermal retrofit concept.

Figure 3 illustrates the installation sequence of the exoskeleton system, while Fig. 4 presents the strengthened model equipped with the exoskeleton.

Experimental activities. As part of the experimental programme, two geometrically scaled (1:3) reinforced concrete specimens, denoted Model X and Model Y, were constructed with identical geometric and mechanical characteristics. The specimens were conceived as lumped-mass physical models with artificial mass simulation, designed according to the laws of dynamic similitude for shake-table testing to ensure consistent scaling relationships between the prototype and the reduced-scale model.

The testing sequence was organised into three phases to evaluate the performance of the exoskeleton system under different structural conditions. This approach allowed comparison between the behaviour of an initially unstrengthened structure, the effectiveness of post-damage retrofitting, and the performance of a structure strengthened from the beginning.

- Phase 1: The unstrengthened specimen (Model Y) was subjected to progressively increasing seismic excitations until the target displacement demands were reached and significant structural damage, including collapse of the masonry infills, was observed (Fig. 5a). Damage progression was assessed after each excitation level through visual inspection of the reinforced concrete members and masonry infills, supported by the measured structural response. The evolution of the fundamental frequency was evaluated after each test as an indicator of the progressive reduction in structural stiffness, while the strain gauges were continuously monitored throughout the tests to identify high strain levels in critical regions.
- Phase 2: Prior to Phase 2, only the collapsed first-storey masonry infills were reconstructed, whereas no repair or strengthening of the reinforced concrete members or reinforcement was carried out before installation of the retrofit system (Fig. 5b). The exoskeleton system was then installed on the previously damaged Model Y, and the specimen was retested to assess the recovery of strength, stiffness and ductility, as well as the interaction between the exoskeleton and the infill walls.
- Phase 3: A second specimen (Model X), pre-strengthened with the exoskeleton from the beginning, was tested under the same seismic inputs to enable direct comparison between preventive strengthening and post-damage retrofitting configurations (Fig. 5c).

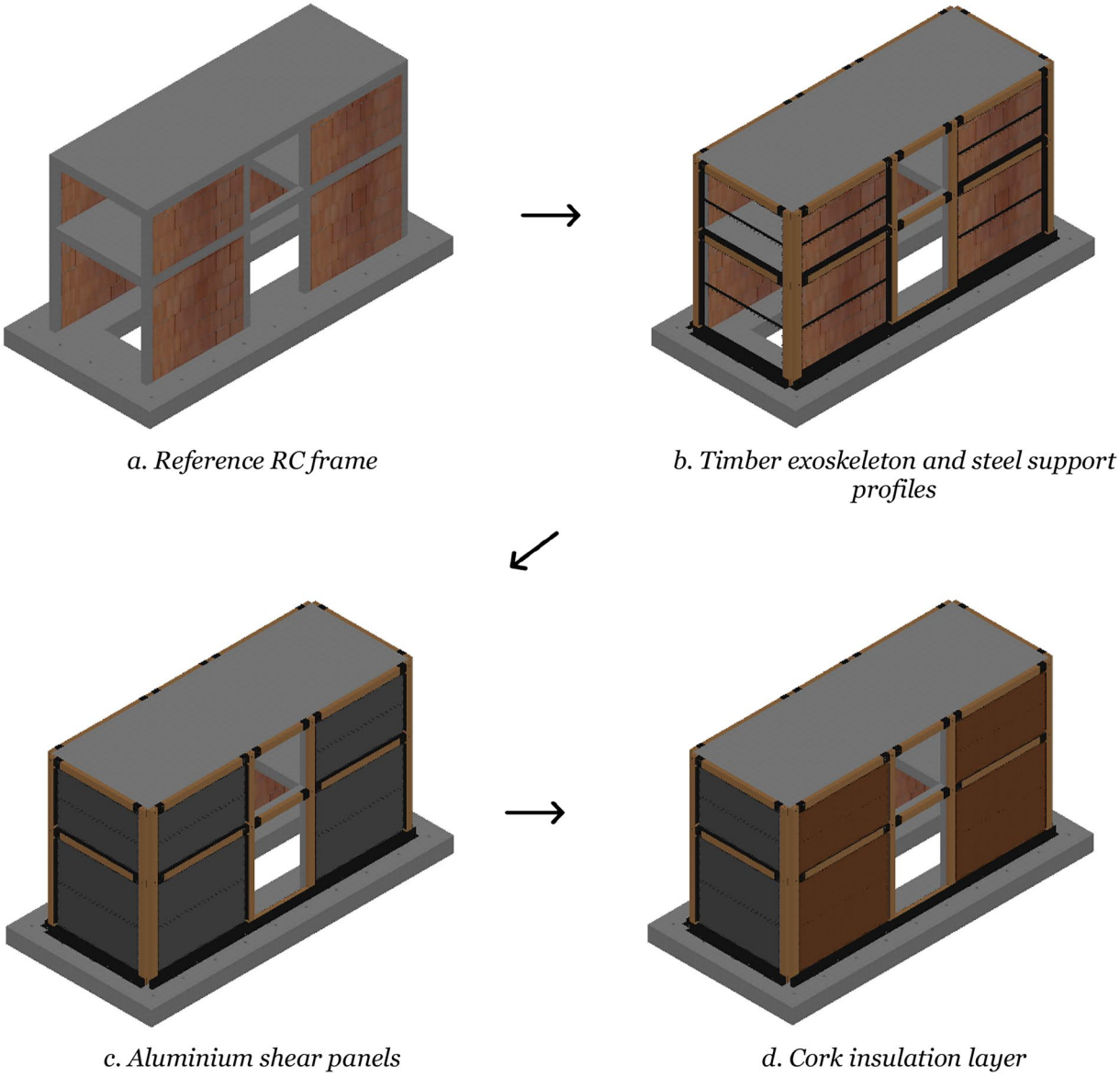
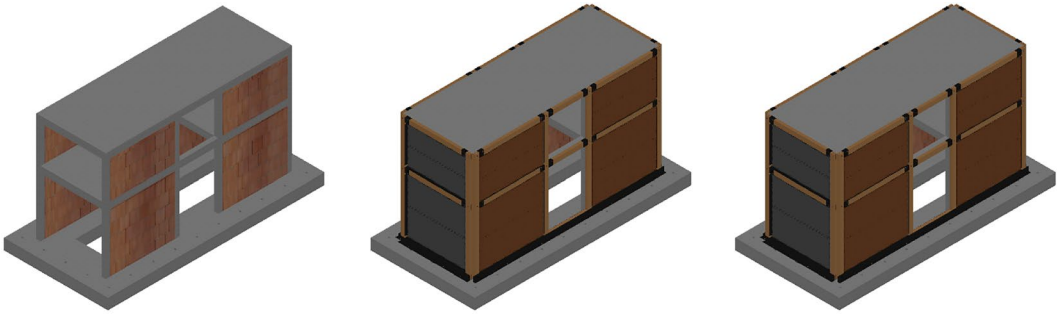


Fig. 3 Exoskeleton installation sequence.



Fig. 4 RC model strengthened with the exoskeleton system.



a. Phase 1 – Model Y *b. Phase 2 – Model Y* *c. Phase 3 – Model X*

Fig. 5 Experimental testing phases of Model X and Model Y.

Material	Property	Value	Standard/Source
Reinforcement bars	Yield strength (Φ4)	697.4 MPa	MKC EN 15630-1
	Ultimate strength (Φ4)	739.3 MPa	
	Yield strength (Φ6)	339.3 MPa	
	Ultimate strength (Φ6)	428.6 MPa	
	Yield strength (Φ8)	570.0 MPa	
	Ultimate strength (Φ8)	682.1 MPa	
	Yield strength (Φ10)	573.9 MPa	
	Ultimate strength (Φ10)	673.9 MPa	
Aluminium panels	Tensile strength	168.3 MPa	MKC C.A4.002
	Breaking strength	229.2 MPa	
Steel connectors/angles	Tensile strength	411.7 MPa	MKC C.A4.002
	Breaking strength	552.5 MPa	
Masonry units	Compressive strength (parallel to holes)	5.71 MPa	MKC EN 771-1; EN 772-1
	Compressive strength (perpendicular)	1.40 MPa	
Mortar	Flexural strength	2.62 MPa	MKC 13412
	Compressive strength	9.63 MPa	
	Modulus of elasticity	16.4 GPa	
Concrete	Compressive strength	22.9 MPa	MKC EN 12390-3; -13
	Modulus of elasticity	26.8 GPa	

Table 2. Measured mechanical properties of the materials.

Materials characterisation tests. The models were designed using concrete class C16/20 and reinforcement steel grade B450C. To verify the actual material properties, a series of laboratory tests were carried out:

- Compressive strength of concrete, testing method MKS EN 12390-3:2019[42] (Report No. ABK – 10/24-1237);
- Modulus of elasticity of concrete, testing method MKS EN 12390-13:2014[43] (Report No. ABK – 10/24-1238);
- Mechanical and physical properties of reinforcement bars (yield and ultimate strengths), testing method MKS EN ISO 15630-1:2011, Clause 5[44] (Report No. ABK – 02/25-215);
- Mechanical properties of structural steel and aluminium elements, testing method MKS C.A4.002[45] (Report No. ABK – 02/25-216);
- Compressive strength of masonry units (block 10, 250 × 250 × 100 mm), testing methods MKS EN 771-1:2011 + A1:2016[46] and MKS EN 772-1:2013 + A1:2015[47] (Report No. AGI – 10/24-1167);
- Compressive strength and modulus of elasticity of mortar (MM50), testing method MKS EN 13412[48] (Report No. ABK – 11/24-1428).

The principal measured mechanical properties of the materials used in the experimental specimens are summarised in Table 2.

For the laminated timber elements, no additional laboratory tests were carried out, as the mechanical properties were defined based on manufacturer-provided certification and accompanying technical documentation.

All laboratory reports are included in the published dataset.

Instrumentation and transducer specifications. The shaking table tests were conducted at the Dynamic Testing Laboratory of the Institute of Earthquake Engineering and Engineering Seismology (IZIIS), Skopje, North Macedonia. The facility consists of a 5.0 m × 5.0 m pre-stressed concrete waffle slab with a self-weight of 33 tons and a payload capacity of up to 40 tons. The table provides five degrees of freedom through two lateral and four vertical MTS hydraulic actuators, controlled by an MTS Digital Controller 469D. Data acquisition was performed using a National Instruments PXI modular system.

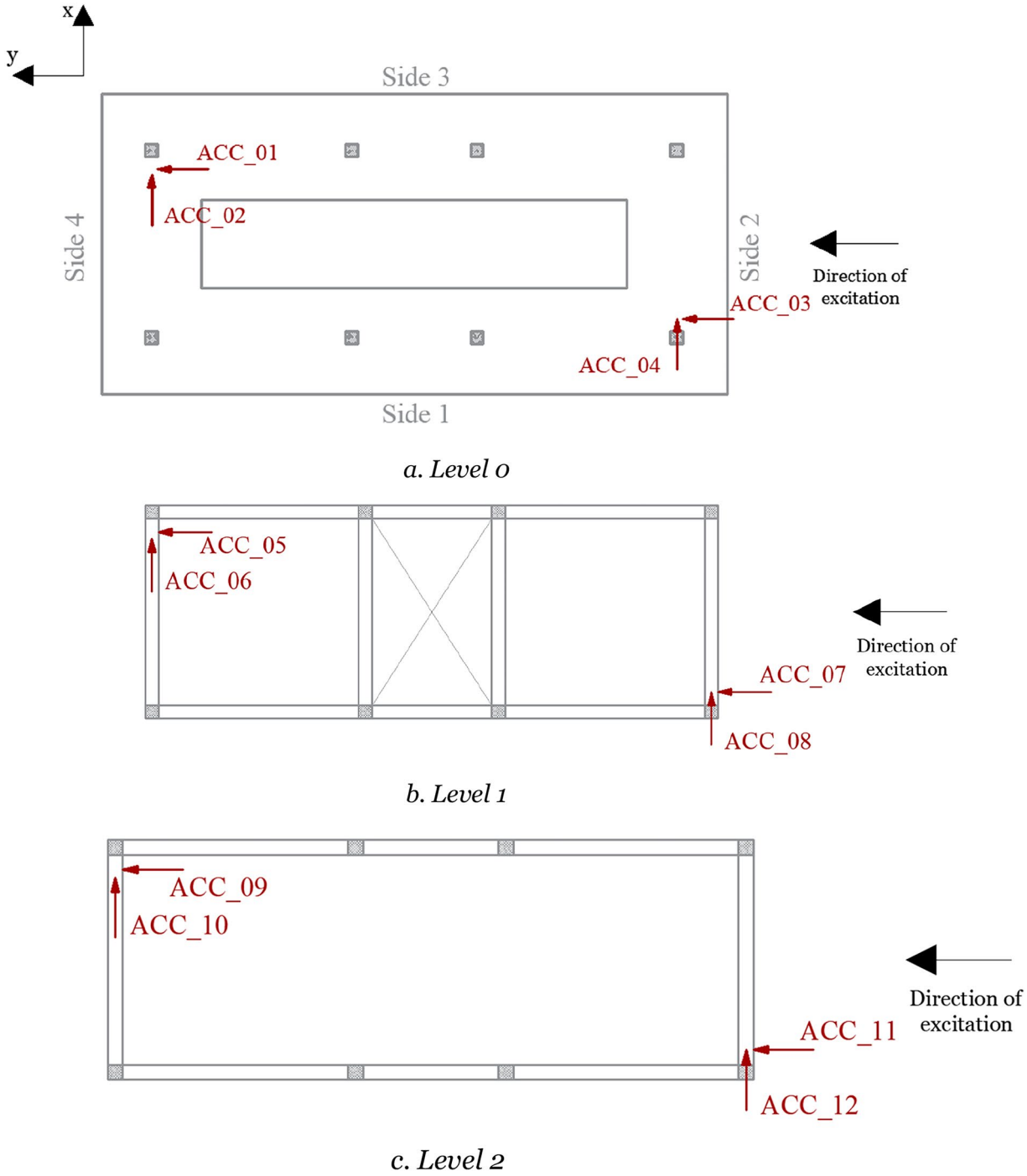


Fig. 6 Accelerometers (ACC) on concrete frame.

To monitor the structural response, multiple sensor types were installed, including accelerometers (ACCs, PCB Piezotronics), linear potentiometers (LPs, Micro-Epsilon WDS), linear variable differential transformers (LVDTs, MacroSensors DC750) and strain gauges (SGs, KYOWA KFG). These instruments recorded accelerations, absolute and relative displacements, and strains throughout the experimental campaign.

The instrumentation layout comprised 15 accelerometers installed at different elevations and in two horizontal directions. Four linear potentiometers were positioned at slab levels. Ten LVDTs were used, including two measuring relative displacement between the model and the shaking table and eight installed around beam–to-column joints. In addition, 30 strain gauges were mounted, with 24 attached to reinforcement bars in the columns at various heights and six installed on the concrete surface. Strain gauge recordings are provided as separate data files within the dataset.

Figures 6–11 present the complete instrumentation layout for all testing phases, while Table 3 specifies the exact position of each transducer and indicates the active sensors during each phase. Column labels referenced in Table 3 are defined in Fig. 1.

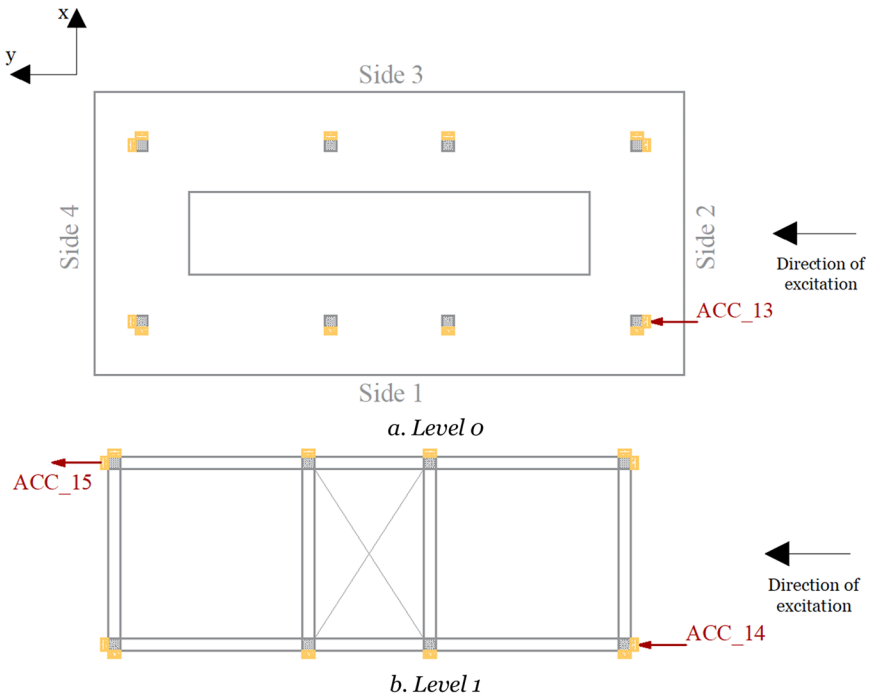


Fig. 7 Accelerometers (ACC) on timber frame.

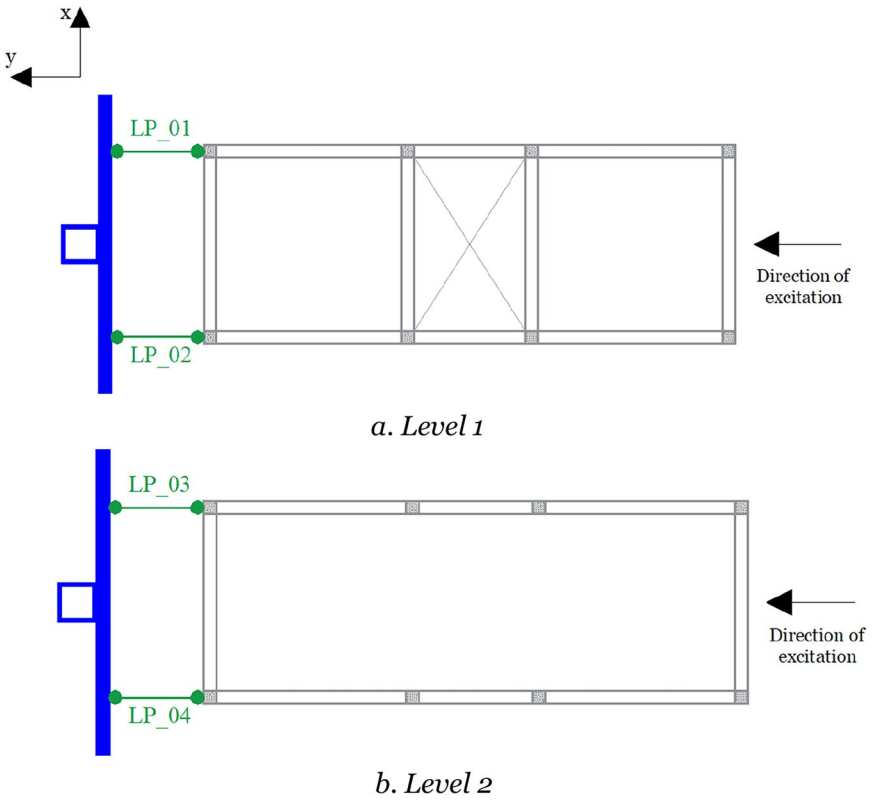


Fig. 8 Linear potentiometers (LPs).

Testing program. The experimental campaign comprised 66 performed tests, organised into three phases. A consistent testing protocol was applied throughout all phases, incorporating two types of excitation: resonant frequency tests and seismic excitation tests. Resonant frequency tests were conducted to determine the dynamic characteristics of the specimens and were performed at the initial state, after selected seismic tests, and at the end of each phase.

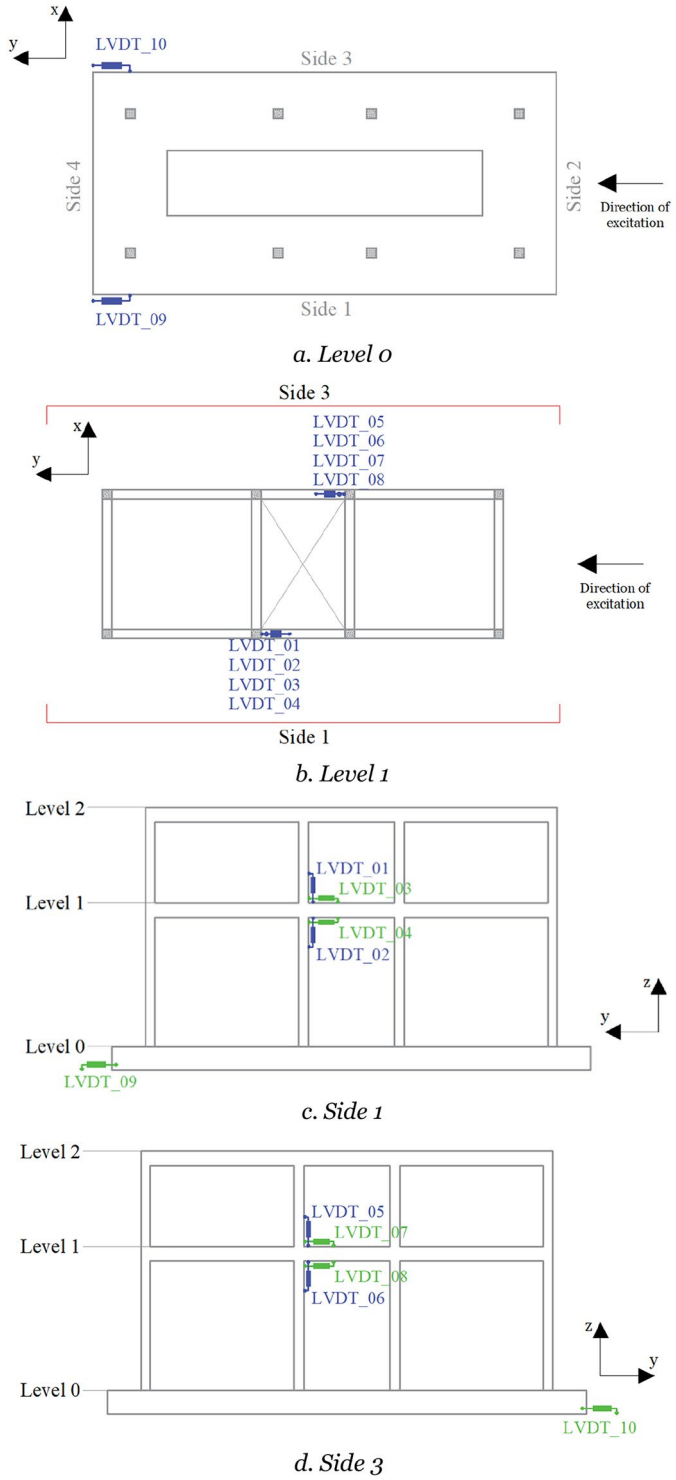


Fig. 9 Linear variable differential transformers (LVDT).

To evaluate seismic performance under simulated earthquake loading, three input records were selected: EQ. 1 (Adana, 1998, Mw 6.3), EQ. 2 (synthetic record generated in accordance with the Eurocode 8 spectrum for Soil Type C), and EQ. 3 (Umbria, 2016, Mw 6.2) (Fig. 12). The selected motions were chosen based on their spectral characteristics and frequency content, representative of the expected seismic demand for the considered building typology.

The ground motions were scaled according to the 1:3 similitude requirements of the physical model. Time scaling followed the relation $t_{model} = t_{prototype}/\sqrt{3}$, while amplitude scaling was applied to define the excitation levels used in each phase. The maximum intensity differed depending on the structural condition of the tested configuration. Complete lists of all tests performed in Phases 1, 2 and 3 are provided in Tables 4–6.

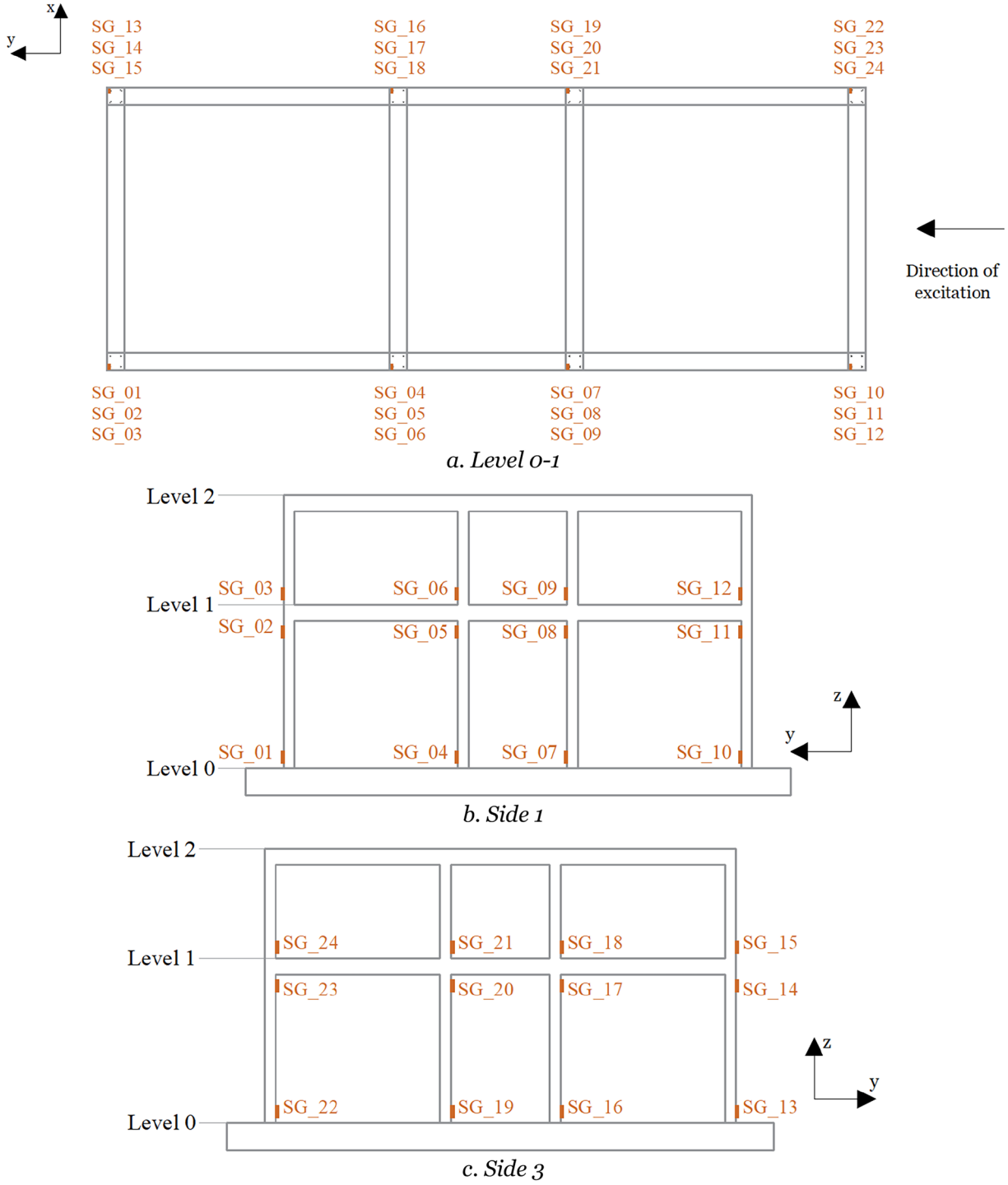


Fig. 10 Strain gauges (SG) on reinforcing bar.

Data Records

The complete dataset generated within the ERIES–RESUME shaking table experimental campaign is publicly available through the Built Environment Data: Experiments repository[49]. The data are released under the Creative Commons Attribution 4.0 International (CC BY 4.0), permitting unrestricted use, distribution and reproduction provided appropriate credit is given.

The repository is organised into four main folders, accompanied by the full technical project report.

The folder "Geometrical Characteristic and Instrumentation" contains documentation describing the geometry of the tested specimens, structural configuration and instrumentation layout adopted during the shaking table campaign. This folder provides the metadata necessary for interpretation of the recorded signals and reconstruction of the experimental setup.

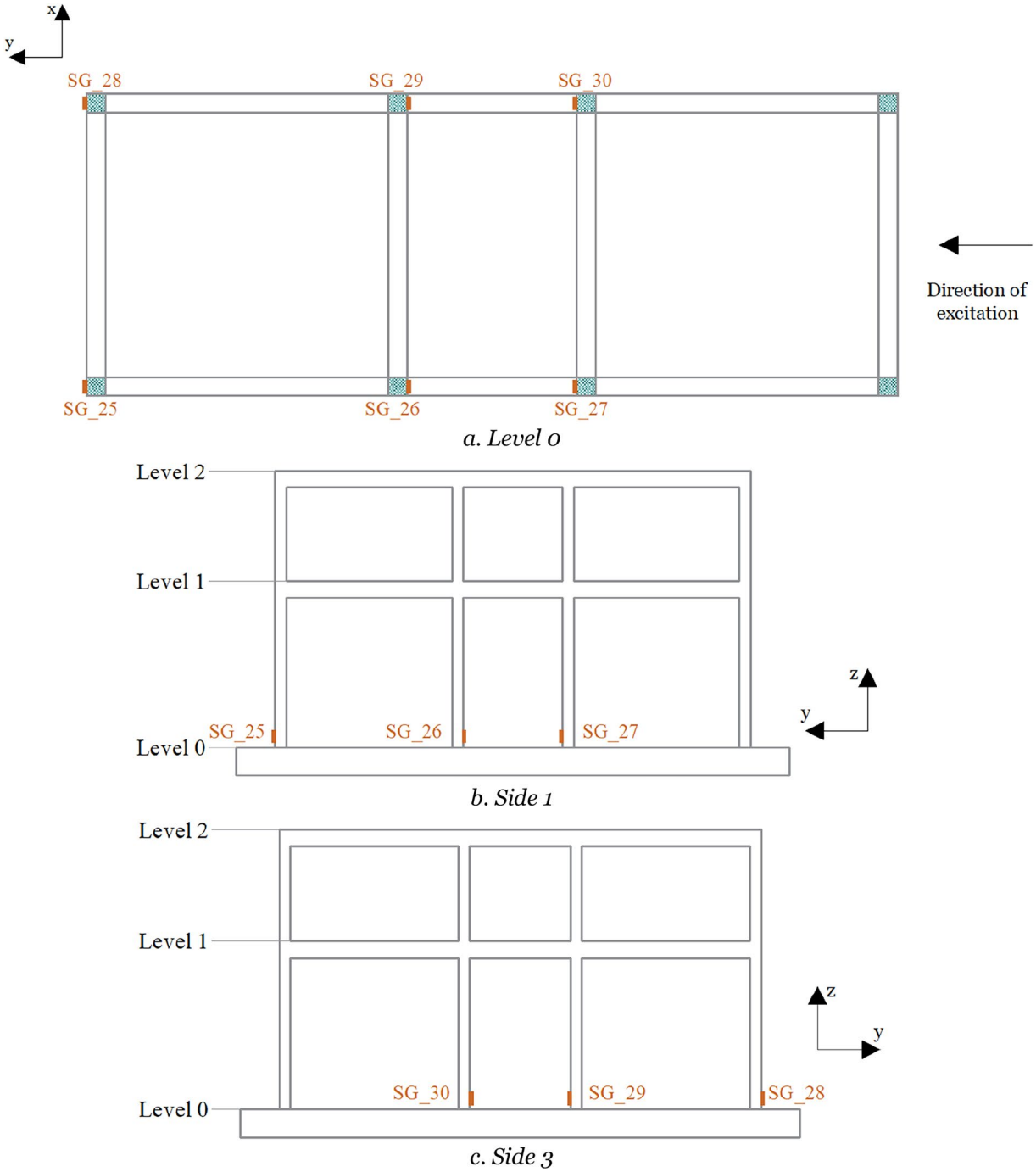


Fig. 11 Strain gauges (SG) on concrete.

The folder "Material Testing Reports" includes the complete laboratory reports used for material characterisation, providing the reference mechanical properties of the concrete, reinforcement steel, masonry units, timber, steel and aluminium elements incorporated in the experimental models.

The folder "Photos and Videos" contains visual documentation of the construction stages, installation of the exoskeleton system and the different phases of dynamic testing.

The folder "Results – Shaking Table" provides the measured time-history data obtained during the experimental programme. The records are provided in TDM format, with one file corresponding to each individual test and organised by testing phase. Each file contains synchronised time-history records from the installed instrumentation, including accelerometers, displacement transducers and strain gauges. The TDM files can be accessed using National Instruments software or imported into Microsoft Excel using the dedicated TDM plug-in. All channels were time-synchronised and acquired at a constant sampling frequency of 1000 Hz. The files preserve the original data organisation adopted during the experimental campaign and include the corresponding channel metadata and measurement units. Acceleration, displacement and strain measurements

Channel name	Type of transducer	Measured quantity (units)	Position	Phase 1	Phase 2	Phase 3
				On/off	On/off	On/off
ACC 1	Accelerometer	Acceleration (g)	Column S5 - Level 0, horizontal dir. (+y)	On	On	On
ACC 2			Column S5 - Level 0, horizontal dir. (+x)	On	On	On
ACC 3			Column S4 - Level 0, horizontal dir. (+y)	On	On	On
ACC 4			Column S4 - Level 0, horizontal dir. (+x)	On	On	On
ACC 5			Column S5 - Level 1, horizontal dir. (+y)	On	On	On
ACC 6			Column S5 - Level 1, horizontal dir. (+x)	On	On	On
ACC 7			Column S4 - Level 1, horizontal dir. (+y)	On	On	On
ACC 8			Column S4 - Level 1, horizontal dir. (+x)	On	On	On
ACC 9			Column S5 - Level 2, horizontal dir. (+y)	On	On	On
ACC 10			Column S5 - Level 2, horizontal dir. (+x)	On	On	On
ACC 11			Column S4 - Level 2, horizontal dir. (+y)	On	On	On
ACC 12			Column S4 - Level 2, horizontal dir. (+x)	On	On	On
ACC 13			Column S4 (timber frame) - Level 0, horizontal dir. (+y)	Off	On after test 30	On
ACC 14			Column S4 (timber frame) - Level 1, horizontal dir. (+y)	Off	On after test 30	On
ACC 15			Column S5 (timber frame) - Level 1, horizontal dir. (+y)	Off	On after test 30	On
LVDT 1	linear variable differential transformer	Relative displacement (mm)	Above beam-column S2 joint, vertical dir. (z)	On	On	On
LVDT 2			Below beam-column S2 joint, vertical dir. (z)	On	On	On
LVDT 3			Above beam-column S2 joint, horizontal dir. (y)	On	On	On
LVDT 4			Below beam-column S2 joint, horizontal dir. (y)	On	On	On
LVDT 5			Above beam-column S7 joint, vertical dir. (z)	On	On	On
LVDT 6			Below beam-column S7 joint, vertical dir. (z)	On	On	On
LVDT 7			Above beam-column S7 joint, horizontal dir. (y)	On	On	On
LVDT 8			Below beam-column S7 joint, horizontal dir. (y)	On	On	On
LVDT 9			Foundation (right side) - shake table, horizontal dir. (y)	On	On	On
LVDT 10			Foundation (left side) - shake table, horizontal dir. (y)	On	On	On
LP1	Linear potentio-meter	Absolute displacement (mm)	Column S5 - Level 1, horizontal dir. (y)	On	On	On
LP2			Column S1 - Level 1, horizontal dir. (y)	On	On	On
LP3			Column S5 - Level 2, horizontal dir. (y)	On	On	On
LP4			Column S1 - Level 2, horizontal dir. (y)	On	On	On
SG1	Strain Gauge	Strain (μstr)	Column S1, Above foundation, Rebar, horizontal dir. (y)	On	On	On
SG2			Column S1, Below beam-column joint Rebar, horizontal dir. (y)	On	On	On
SG3			Column S1, Above beam-column joint, Rebar, horizontal dir. (y)	On	On	On
SG4			Column S2, Above foundation, Rebar, horizontal dir. (y)	On	On	On
SG5			Column S2, Below beam-column joint Rebar, horizontal dir. (y)	On	On	On
SG6			Column S2, Above beam-column joint, Rebar, horizontal dir. (y)	On	On	On
SG7			Column S3, Above foundation, Rebar, horizontal dir. (y)	On	On	On
SG8			Column S3, Below beam-column joint Rebar, horizontal dir. (y)	On	On	On
SG9			Column S3, Above beam-column joint, Rebar, horizontal dir. (y)	On	On	On
SG10			Column S4, Above foundation, Rebar, horizontal dir. (y)	On	On	On
SG11			Column S4, Below beam-column joint Rebar, horizontal dir. (y)	On	On	On
SG12			Column S4, Above beam-column joint, Rebar, horizontal dir. (y)	On	On	On
SG13			Column S5, Above foundation, Rebar, horizontal dir. (y)	On	On	On
SG14			Column S5, Below beam-column joint Rebar, horizontal dir. (y)	On	On	On
SG15			Column S5, Above beam-column joint, Rebar, horizontal dir. (y)	On	On	On
SG16			Column S6, Above foundation, Rebar, horizontal dir. (y)	On	On	On
SG17			Column S6, Below beam-column joint Rebar, horizontal dir. (y)	On	On	On
SG18			Column S6, Above beam-column joint, Rebar, horizontal dir. (y)	On	On	On
SG19			Column S7, Above foundation, Rebar, horizontal dir. (y)	On	On	On
SG20			Column S7, Below beam-column joint Rebar, horizontal dir. (y)	On	On	On
SG21			Column S7, Above beam-column joint, Rebar, horizontal dir. (y)	On	On	On
SG22			Column S8, Above foundation, Rebar, horizontal dir. (y)	On	On	On
SG23			Column S8, Below beam-column joint Rebar, horizontal dir. (y)	On	On	On
SG24			Column S8, Above beam-column joint, Rebar, horizontal dir. (y)	On	On	On
SG25			Column S1, Above foundation, Concrete, horizontal dir. (y)	On	Off	Off
SG26			Column S2, Above foundation, Concrete, horizontal dir. (y)	On	Off	On
SG27			Column S3, Above foundation, Concrete, horizontal dir. (y)	On	Off	On
SG28			Column S5, Above foundation, Concrete, horizontal dir. (y)	On	Off	Off
SG29			Column S6, Above foundation, Concrete, horizontal dir. (y)	On	Off	On
SG30			Column S7, Above foundation, Concrete, horizontal dir. (y)	On	Off	On

Table 3. Location of the transducers.

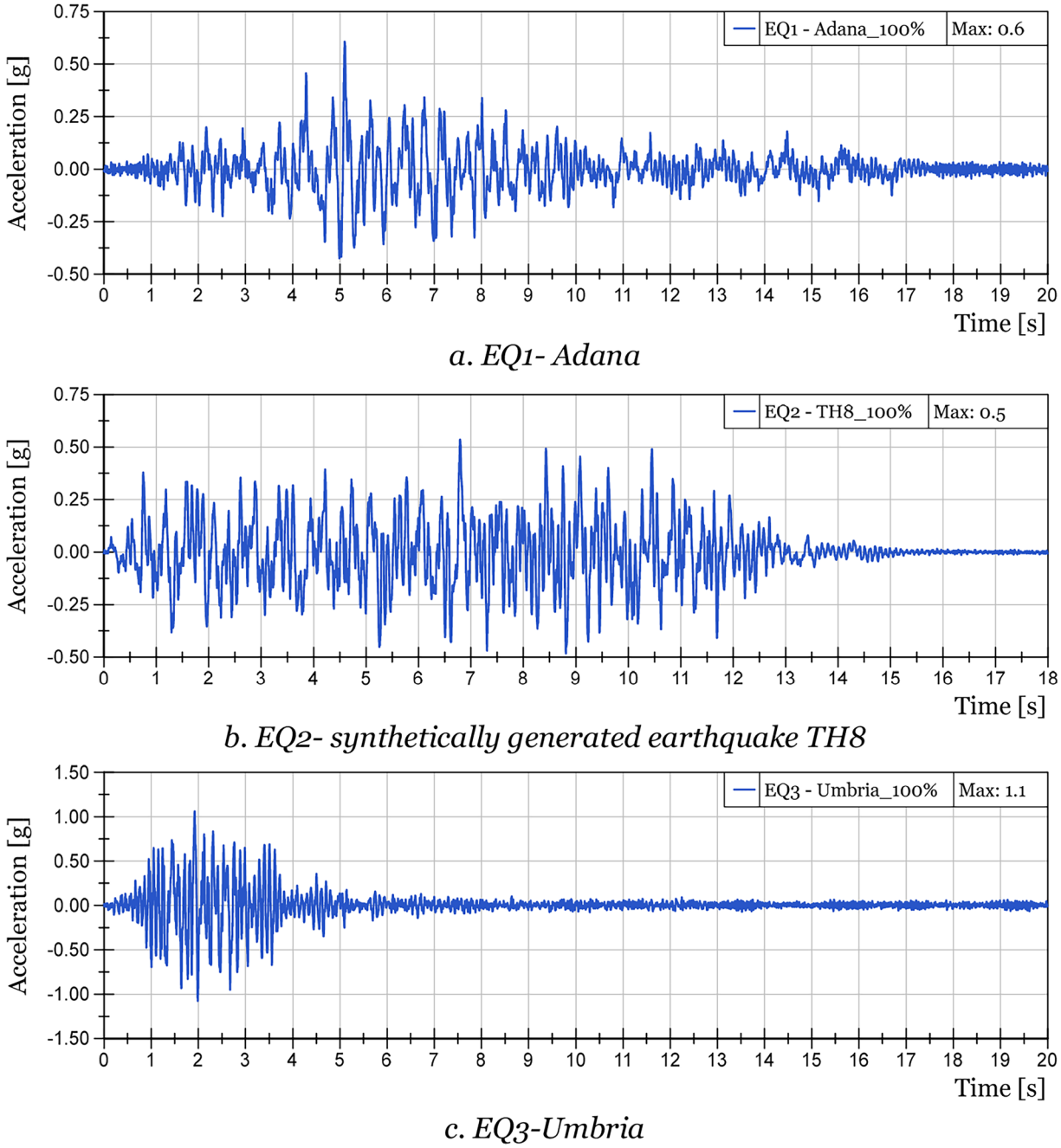


Fig. 12 Time history record of selected ground motions.

are reported in g, mm and με (microstrain), respectively. Channel names follow the sensor identification convention adopted throughout the manuscript, allowing direct association with the instrumentation layout presented in Figs. 6–11. Individual channels are labelled according to the corresponding sensor type and number (e.g., ACC01–ACC12, LP01–LP04 and LVDT01–LVDT10, SG01-30). In addition to the structural response channels, the files include shaking-table system channels. The labels SYS DIS-Y/Z Fbk and SYS ACC-Y/Z Fbk denote the horizontal (Y) and vertical (Z) feedback displacement and acceleration signals, respectively, while SYS ACC-Y/Z CST correspond to the accelerations measured at the centre of the shaking table. The channels Lat Reference and Vert Reference contain the commanded lateral and vertical reference acceleration signals applied to the shaking table. The released records correspond to the processed signals used throughout the experimental campaign. Prior to publication, the acceleration records were high-pass filtered with a cut-off frequency of 0.5 Hz to remove low-frequency drift and correct minor direct current (DC) offsets. The displacement and strain records are provided in their original recorded form. No additional post-processing was applied to the released dataset.

Test No.	Type of excitation	Characteristics of the excitation	Input acc. [g]
1	Random	f = 1-45.0 Hz; t = 300 s	0.01
2	Random	f = 1-45.0 Hz; t = 300 s	0.02
3	Random	f = 1-45.0 Hz; t = 300 s	0.05
4	EQ. 1: Adana	15%	0.09
5	EQ. 2: TH8_scaled	18%	0.1
6	EQ. 3: Umbria	10%	0.13
7	EQ. 2: TH8_scaled	27%	0.15
8	EQ. 2: TH8_scaled	50%	0.26
9	Random	f = 1-45.0 Hz; t = 300 s	0.05
10	EQ. 2: TH8_scaled	75%	0.35
11	Random	f = 1-45.0 Hz; t = 300 s	0.05
12	EQ. 2: TH8_scaled	100%	0.51
13	Random	f = 1-45.0 Hz; t = 300 s	0.05
14	EQ. 2: TH8_scaled	100%	0.51
15	Random	f = 1-45.0 Hz; t = 300 s	0.05
16	EQ. 2: TH8_scaled	120%	0.54
17	Random	f = 1-45.0 Hz; t = 300 s	0.05
18	EQ. 2: TH8_scaled	140%	0.65
19	Random	f = 1-45.0 Hz; t = 300 s	0.02

Table 4. List of performed tests - Phase 1.

Test No.	Type of excitation	Characteristics of the excitation	Input acc. [g]
20	Random	f = 1-45.0 Hz; t = 300 s	0.05
21	EQ. 1: Adana	15%	0.09
22	EQ. 2: TH8_scaled	18%	0.08
23	EQ. 3: Umbria	10%	0.1
24	EQ. 2: TH8_scaled	27%	0.12
25	EQ. 2: TH8_scaled	50%	0.23
26	Random	f = 1-45.0 Hz; t = 300 s	0.05
27	EQ. 2: TH8_scaled	75%	0.34
28	Random	f = 1-45.0 Hz; t = 300 s	0.05
29	EQ. 2: TH8_scaled	100%	0.44
30	Random	f = 1-45.0 Hz; t = 300 s	0.05
31	EQ. 2: TH8_scaled	120%	0.52
32	Random	f = 1-45.0 Hz; t = 300 s	0.05
33	EQ. 2: TH8_scaled	140%	0.65
34	Random	f = 1-45.0 Hz; t = 300 s	0.05
35	EQ. 2: TH8_scaled	160%	0.76
36	Random	f = 1-45.0 Hz; t = 300 s	0.05
37	EQ. 2: TH8_scaled	180%	0.9
38	Random	f = 1-45.0 Hz; t = 300 s	0.05

Table 5. List of performed tests - Phase 2.

In addition, the repository includes the document "ERIES-RESUME_Report IZIIS.pdf", which provides extended technical documentation of the experimental campaign, instrumentation configuration and testing programme, supporting interpretation and reuse of the dataset.

Technical Validation

All ACCs, LVDTs, LPs and SGs were calibrated as part of the laboratory's annual calibration programme by comparison with reference instruments verified at an officially accredited metrology laboratory, ensuring measurement traceability. For each sensor type, one reference sensor calibrated at the accredited laboratory was used to perform a comparative calibration of the remaining sensors under identical loading conditions. Individual calibration coefficients were determined for each instrument and applied during data acquisition to convert the measured electrical signals into the corresponding physical quantities, ensuring the accuracy and consistency of the recorded measurements.

Test No.	Type of excitation	Characteristics of the excitation	Input acc. [g]
39	Random	f = 1-45.0 Hz; t = 300 s	0.05
40	EQ. 1: Adana	15%	0.09
41	EQ. 2: TH8_scaled	18%	0.12
42	EQ. 3: Umbria	10%	0.11
43	EQ. 2: TH8_scaled	27%	0.15
44	EQ. 2: TH8_scaled	50%	0.27
45	Random	f = 1-45.0 Hz; t = 300 s	0.05
46	Random	f = 1-45.0 Hz; t = 300 s	0.05
47	EQ. 2: TH8_scaled	75%	0.39
48	Random	f = 1-45.0 Hz; t = 300 s	0.05
49	EQ. 2: TH8_scaled	100%	0.50
50	Random	f = 1-45.0 Hz; t = 300 s	0.05
51	EQ. 2: TH8_scaled	120%	0.55
52	Random	f = 1-45.0 Hz; t = 300 s	0.05
53	EQ. 2: TH8_scaled	140%	0.63
54	Random	f = 1-45.0 Hz; t = 300 s	0.05
55	EQ. 2: TH8_scaled	160%	0.75
56	Random	f = 1-45.0 Hz; t = 300 s	0.05
57	EQ. 2: TH8_scaled	180%	0.94
58	Random	f = 1-45.0 Hz; t = 300 s	0.05
59	EQ. 2: TH8_scaled	200%	1.14
60	Random	f = 1-45.0 Hz; t = 300 s	0.05
61	Random	f = 4-12.0 Hz; t = 50 s	0.1
62	Random	f = 4-12.0 Hz; t = 50 s	0.3
63	Random	f = 1-45.0 Hz; t = 300 s	0.05
64	Random	f = 4.8-8.8 Hz; t = 50 s	0.3
65	Random	f = 4-12.0 Hz; t = 50 s	0.3
66	Random	f = 1-45.0 Hz; t = 300 s	0.05

Table 6. List of performed tests - Phase 3.

Before the start of the testing programme, the shaking table system underwent mechanical and control verification. For each test, the target and executed acceleration time histories were first visually compared using the MTS shaking-table control software to verify the correct reproduction of the prescribed input motion. In addition, the similarity between the target and executed acceleration time histories was quantitatively evaluated using cross-correlation analysis, providing objective verification that the reproduced shaking-table motions accurately followed the prescribed input.

During high-intensity excitations, certain sensors reached their measurement limits, resulting in temporary signal saturation. These occurrences were identified during data review and are clearly traceable within the corresponding time-history records. As structural damage progressed, some strain gauges reached their measurement range or became detached or damaged during testing. Their operational status during the different testing phases is documented in Table 3. No data loss occurred, and the overall measurement system remained consistent and coherent.

Signal quality was further assessed through visual inspection of the recorded time histories and frequency-domain analysis to verify the consistency and reliability of the acquired measurements.

Data availability

The complete dataset generated within the ERIES–RESUME shaking table experimental campaign is publicly available through the Built Environment Data: Experiments repository [40]. The data are released under the Creative Commons Attribution 4.0 International (CC BY 4.0), permitting unrestricted use, distribution and reproduction provided appropriate credit is given.The repository is organised into four main folders, accompanied by the full technical project report.The folder “Geometrical Characteristic and Instrumentation” contains documentation describing the geometry of the tested specimens, structural configuration and instrumentation layout adopted during the shaking table campaign. This folder provides the metadata necessary for interpretation of the recorded signals and reconstruction of the experimental setup.The folder “Material Testing Reports” includes the complete laboratory reports used for material characterisation, providing the reference mechanical properties of the concrete, reinforcement steel, masonry units, timber, steel and aluminium elements incorporated in the experimental models.The folder “Photos and Videos” contains visual documentation of the construction stages, installation of the exoskeleton system and the different phases of dynamic testing.The folder “Results – Shaking Table” provides the measured time-history data obtained during the experimental programme. The records are provided in TDM format, with one file corresponding to each individual test and organised by testing phase. Each file contains synchronised measurements from the installed

instrumentation, including accelerometers, displacement transducers and strain gauges. The TDM files can be accessed using National Instruments software or previewed in Microsoft Excel via the dedicated plug-in.In addition, the repository includes the document "ERIES-RESUME_Report IZIIS.pdf", which provides extended technical documentation of the experimental campaign, instrumentation configuration and testing programme, supporting interpretation and reuse of the dataset.

Code availability

No custom code was developed for this study. The dataset is provided in TDM format and can be accessed using National Instruments software. For user convenience, the TDM Excel Add-in supplied by National Instruments is included in the dataset repository, enabling users to import, inspect, visualise and export the recorded data directly within Microsoft Excel without requiring additional custom software.

Received: 10 March 2026; Accepted: 24 September 2026;
Published: xx xx xxxx

References

1. Palermo, V., Tsionis, G., Sousa, M. L. *Building Stock Inventory to Assess Seismic Vulnerability across Europe*. Publications Office of the European Union (2018).
2. Takagi, J. & Wada, A. Recent earthquakes and the need for a new philosophy for earthquake-resistant design. *Soil Dyn. Earthq. Eng.* **119**, 499–507 (2019).
3. Di Bucci, D. *et al. Science for Disaster Risk Management 2020: Acting Today, Protecting Tomorrow*. Publications Office of the European Union (2021).
4. Sheshov, V. *et al.* Reconnaissance analysis on buildings damaged during Durres Earthquake Mw6.4, 26 November 2019, Albania. *Bull. Earthq. Eng.* (2021).
5. United Nations Environment Programme. Global Status Report for Buildings and Construction: Towards a Zero-Emission, Efficient and Resilient Buildings and Construction Sector (2020).
6. European Commission. The European Green Deal (2019).
7. International Energy Agency (IEA). Policy Database (2021).
8. Huo, T. *et al.* China's building stock estimation and energy intensity analysis. *J. Clean. Prod.* **207**, 801–813 (2019).
9. Secretary of State. The Energy Efficiency (Building Renovation and Reporting) Regulations (2020).
10. Caverzan, A., Lamperti Tornaghi, M., Negro, P. (eds). Proceedings of SAFESUST Workshop. Publications Office of the European Union (2016).
11. Marini, A. *et al.* Technology Options for Earthquake Resistant, Eco-Efficient Buildings in Europe. *EUR* **26497** EN (2014).
12. Belleri, A. & Marini, A. Does seismic risk affect the environmental impact of existing buildings? *Energy Build.* **110**, 149–158 (2016).
13. Clemett, N., Carofilis Gallo, W. W., Gabbianelli, G., O'Reilly, G. J. & Monteiro, R. Optimal combined seismic and energy efficiency retrofitting for existing buildings in Italy. *J. Struct. Eng.* **149**, 04022305 https://doi.org/10.1061/(ASCE)ST.1943-541X.0003500 (2023).
14. Pohoryles, D. A., Maduta, C., Bournas, D. A. & Kouris, L. A. Energy performance of existing residential buildings in Europe: A novel approach combining energy with seismic retrofitting. *Energy Build.* **223**, 110024 https://doi.org/10.1016/j.enbuild.2020.110024 (2020).
15. Bournas, D. A. Concurrent seismic and energy retrofitting of RC and masonry building envelopes using inorganic textile-based composites combined with insulation materials. *Compos. Part B* **148**, 166–179 (2018).
16. Gkournelos, P. D., Triantafillou, T. C. & Bournas, D. A. Combined seismic and energy upgrading of existing RC buildings using TRM jacketing and thermal insulation. *Earthq. Struct.* **16**, 625–639 (2019).
17. Kallioras, S., Bournas, D. A., Koutas, L., Molina, F. J. Integrated seismic and energy retrofitting of masonry-infilled RC buildings with textile-reinforced mortar and thermal insulation. *J. Build. Eng.* (2024).
18. Christis, Z. *et al.* Seismic and energy upgrading of existing buildings—full-scale testing of retrofitted masonry-infilled RC frames. *Earthq. Eng. Struct. Dyn.* **52**, 4489–4517 (2023).
19. Margani, G., Evola, G., Tardo, C. & Marino, E. M. Energy, seismic, and architectural renovation of RC framed buildings with prefabricated timber panels. *Sustainability* **12**, 4845 (2020).
20. Badini, L., Ott, S., Aondio, P. & Winter, S. Seismic strengthening of existing RC buildings with external CLT walls hosting integrated energetic renovation. *Bull. Earthq. Eng.* **20**, 5963–6006 (2022).
21. Callegaro, N. & Albatici, R. Energy retrofit with prefabricated timber-based façade modules. *J. Facade Des. Eng.* **11**, 001–018 (2023).
22. Valluzzi, M. R. *et al.* Nested Buildings: An Innovative Strategy for the Integrated Seismic and Energy Retrofit of Existing Masonry Buildings with CLT Panels. *Sustainability* **13**, 1188 (2021).
23. Damiani, N., Guerrini, G. & Graziotti, F. Design procedure for a timber-based seismic retrofit applied to masonry buildings. *Engineering Structures* **301**, 116991 (2024).
24. Liu, J. *et al.* A low-cost timber cladding system for the sustainable retrofit of masonry buildings: mechanical characterization under diagonal compression. *Engineering Structures* **322**, 119099 (2025).
25. Reggio, A., Restuccia, L. & Ferro, G. A. Seismic performance of exoskeleton structures. *Eng. Struct.* **198**, 109459 (2019).
26. Labò, S., Passoni, C., Marini, A. & Belleri, A. Design of diagrid exoskeletons for retrofit of RC buildings. *Eng. Struct.* **220**, 110899 (2020).
27. Cucuzza, R., Aloisio, A., Domaneschi, M., Nascimbene, R. Multimodal seismic assessment of infrastructures retrofitted with exoskeletons. *Bull. Earthq. Eng.* (2024).
28. Olivo, J., Cucuzza, R., Bertagnoli, G., Domaneschi, M. Optimal design of steel exoskeletons via genetic algorithm. *Comput. Struct.* (2024).
29. Formisano, A., Galano, S., Meglio, E., Del Vecchio, C. & Prota, A. Experimental investigation on innovative lightweight steel exoskeleton for seismic resilience of masonry-infilled reinforced concrete frames. *Eng. Struct.* **344**, 121410 https://doi.org/10.1016/j.engstruct.2025.121410 (2025).
30. Formisano, A., Longobardi, G. Seismic fragility and energy efficiency upgrading of masonry compounds using lightweight aluminium alloy exoskeletons: a case study in South Italy. *Bull. Earthq. Eng.* https://doi.org/10.1007/s10518-025-02149-2 (2025).
31. Meglio, E., Longobardi, G. & Formisano, A. Integrated seismic-energy retrofit systems for preventing failure of a historical RC school building: Comparison among metal lightweight exoskeleton solutions. *Eng. Fail. Anal.* **154**, 107663 https://doi.org/10.1016/j.engfailanal.2023.107663 (2023).
32. Ferraioli, M., Lavino, A. & De Matteis, G. A design method for seismic retrofit of RC frame buildings using aluminium shear panels. *Arch. Civ. Mech. Eng.* **23**, 106 (2023).
33. De Matteis, G. & Ferraioli, M. Metal shear panels for seismic upgrading of RC buildings: A case study. *Key Eng. Mater.* **763**, 1058–1066 (2018).

34. Engineering Research Infrastructures for European Synergies (ERIES). Horizon Europe Framework Programme, Grant Agreement No. 101058684 (2022–2026).
35. Formisano, A. *et al.* Seismic performance of a hybrid timber–aluminium exoskeleton for retrofitting RC buildings. *Buildings* **16**, 73 (2026).
36. Shoklarovski, A. *et al.* Experimental investigation of an exoskeleton system for integrated structural and energy retrofitting of reinforced concrete structures. In: Proc. 21st Int. Symp. MASE, Ohrid, North Macedonia (2025).
37. Formisano, A. *et al.* The ERIES_RESUME Project: Results of Experimental Activities. In: Milani G, Magagnini E, Khatir S (eds) *ICSCES 2025, Lecture Notes in Civil Engineering*, **746**, 809–817 (Springer, 2025).
38. Formisano, A. *et al.* The RESUME Project: Numerical Analyses and Laboratory Test. In: *ERIES-IW 2025, Lecture Notes in Civil Engineering*, **718**, 230–242 (Springer, 2025).
39. Formisano, A., Galano, S., Meglio, E., Del Vecchio, C. & Prota, A. Experimental investigation on innovative lightweight steel exoskeleton for seismic resilience of masonry-infilled reinforced concrete frames. *Eng. Struct.* **344**, 121410 (2025).
40. Buckingham, E. On Physically Similar Systems: Illustrations of the Use of Dimensional Equations. *Physical Review* (1914).
41. Moncarz, P. D. & Krawinkler, H. Theory and Application of Experimental Model Analysis in Earthquake Engineering. Report No. 50, John A. *Blume Earthquake Engineering Center, Stanford University* (1981).
42. MKS EN 12390-3. Testing hardened concrete – Part 3: Compressive strength of test specimens (2019).
43. MKS EN 12390-13. Testing hardened concrete – Part 13: Determination of secant modulus of elasticity in compression (2021).
44. MKS EN ISO 15630-1. Steel for the reinforcement and prestressing of concrete – Test methods – Part 1: Reinforcing bars, wire rod and wire (2019).
45. MKS C.A4.002. Concrete – Complementary rules for MKS EN 206 (2015).
46. MKS EN 771-1. Specification for masonry units – Part 1: Clay masonry units (2011).
47. MKS EN 772-1. Methods of test for masonry units – Part 1: Determination of compressive strength (2011).
48. 2006). MKS 13412. Standard methods for the testing of mechanical properties of building materials.
49. ERIES_RESUME – REsilient and SUstainable envelope for vulnerable buildings in seisMic affected areas at the time of climatE crisis. *Built Environment Data: Experiments repository* https://doi.org/10.60756/iziis-adb63c95 (2025).

Acknowledgements

This work was carried out within the ERIES–RESUME project, supported by the Engineering Research Infrastructures for European Synergies (ERIES) project (www.eries.eu), which has received funding from the European Union's Horizon Europe Framework Programme under Grant Agreement No. 101058684. The authors acknowledge the valuable contributions of the experts and technical staff whose support was essential for the successful implementation of the experimental campaign.

Author contributions

Antonio Formisano served as Principal Investigator of the project and was responsible for conceptualization, funding acquisition, coordination of the experimental campaign, and overall supervision of the research activities, with support from Marco Domaneschi, Emilia Meglio, and the other co-authors from the partner research groups.Antonio Shoklarovski coordinated the experimental campaign and contributed to the development of the experimental methodology, with support from Aleksandra Bogdanovic and the other co-authors from the hosting institution.Igor Markovski and Nikola Naumovski carried out the experimental tests, while Dejan Filipovski supervised the data acquisition system and performed data processing.Antonio Shoklarovski curated the dataset and prepared the initial draft of the manuscript together with Angela Poposka, Filip Manojlovski, Dejan Ivanovski, and Toni Kitanovski.All authors contributed to the writing and critical revision of the manuscript and approved the final version.

Funding

This work was supported by the ERIES project – Engineering Research Infrastructures for European Synergies (2022–2026), funded by the European Union under the Horizon Europe Framework Programme, Grant Agreement No. 101058684.

Competing interests

The authors declare no competing interests.

Additional information

Correspondence and requests for materials should be addressed to A.S. or M.D.

Reprints and permissions information is available at www.nature.com/reprints.

Publisher's note Springer Nature remains neutral with regard to jurisdictional claims in published maps and institutional affiliations.

Open Access This article is licensed under a Creative Commons Attribution 4.0 International License, which permits use, sharing, adaptation, distribution and reproduction in any medium or format, as long as you give appropriate credit to the original author(s) and the source, provide a link to the Creative Commons licence, and indicate if changes were made. The images or other third party material in this article are included in the article's Creative Commons licence, unless indicated otherwise in a credit line to the material. If material is not included in the article's Creative Commons licence and your intended use is not permitted by statutory regulation or exceeds the permitted use, you will need to obtain permission directly from the copyright holder. To view a copy of this licence, visit http://creativecommons.org/licenses/by/4.0/.

© The Author(s) 2026

This Article in Press is shared early to give you faster access to new research. It is citable and carries a permanent DOI. The final edited version will replace it automatically.